

Effect of Sm and Fe Co-Doping on Structural and Electrical Properties of CeO₂ Solid Electrolyte

Nur Fathin Syuhada Samsudin^{1,2}, Salmie Suhana Che Abdullah^{1,}, Imaduddin Helmi Wan Nordin³, Norzarulasri Kamis³*

*¹Faculty of Chemical Engineering & Technology, Universiti Malaysia Perlis
Kompleks Pusat Pengajian Jejawi 2, 02600 Arau, Perlis, Malaysia*

*²Centre of Excellent For Frontier Materials Research (Frontmate), Universiti
Malaysia Perlis, Jalan Kangar-Alor Setar, Kampung Seriap, 01000 Kangar, Perlis
Malaysia*

*³Faculty of Mechanical Engineering & Technology, Universiti Malaysia Perlis
Kampus Tetap Pauh Putra, 02600 Arau, Perlis, Malaysia*

** Corresponding author; email: salmie@unimap.edu.my*

Received: 22 August 2024 / Accepted: 29 November 2024

ABSTRACT

High efficiency and environmental-benign characteristics of solid oxide fuel cell (SOFC) as an energy source have been receiving enormous attention to overcome global warming, pollution and fuel availability issues. Intensive research in SOFC focuses on developing cells that have high electrochemical performances and durability. The solid electrolyte that is commonly studied as a candidate for SOFC is samarium doped ceria (SDC) because it has higher oxygen ionic conductivity compared to yttria stabilized zirconia (YSZ). In this project, compositional modification of cerium oxide (CeO₂) by single and double substitution of samarium oxide (Sm₂O₃) and iron oxide (Fe₂O₃) with composition of Ce_{0.8}Sm_{0.2}O_{1.9}, Ce_{0.8}Sm_{0.1}Fe_{0.1}O_{1.9} and Ce_{0.7}Fe_{0.1}Sm_{0.2}O_{1.85} were studied. Samples were synthesized via conventional solid state reaction method by mixing the raw materials which is cerium oxide (CeO₂), samarium oxide (Sm₂O₃) and iron oxide (Fe₂O₃), then pressed into pellet, and finally sintered in the range of 1400 °C to 1500 °C. X-ray diffraction (XRD) analysis for phase confirmation and impedance measurement for electrical conductivity were used in order to investigate the influences of the double dopants on the crystal structure and electrical properties. Optimum sintering temperature for sample in this study is 1480 °C. However, at this temperature, single phase was not obtained for Ce_{0.7}Sm_{0.2}Fe_{0.1}O_{1.85} so this sample required different sintering profile. Ce_{0.8}Sm_{0.2}O_{1.9} and Ce_{0.8}Sm_{0.1}Fe_{0.1}O_{1.9} samples show relative density above 97%. Ce_{0.7}Sm_{0.2}Fe_{0.1}O_{1.85} sample shows highest conductivity, which is 0.613 Ω⁻¹m⁻¹ at 600 °C, followed by Ce_{0.8}Sm_{0.2}O_{1.9} (0.350 Ω⁻¹m⁻¹) then Ce_{0.8}Sm_{0.1}Fe_{0.1}O_{1.9} (0.180 Ω⁻¹m⁻¹). Ce_{0.8}Sm_{0.1}Fe_{0.1}O_{1.9} sample has highest activation energy compared to Ce_{0.8}Sm_{0.1}O_{1.9} and Ce_{0.7}Sm_{0.2}Fe_{0.1}O_{1.85} which is 1.255 eV, while Ce_{0.8}Sm_{0.2}O_{1.9} is 0.828 eV and the lowest activation energy is Ce_{0.7}Sm_{0.2}Fe_{0.1}O_{1.85} sample with 0.671 eV.

Keywords: solid oxide fuel cell; double dopant; samarium doped ceria (SDC); solid electrolyte; conductivity

INTRODUCTION

Fuel cells produce efficient and clean electricity by using the chemical energy by hydrogen or other fuel to ensure a friendly environment and pollution free. Humphry Davy introduced the fuel cell concept in the early 19 century [1]. There are six different of fuel cells which are phosphoric acid fuel cell (PAFC), molten carbonate fuel cell (MCFC), proton exchange membrane fuel cell (PEMFC), direct methanol fuel cell (DMFC), and solid oxide fuel cell (SOFC) [2,3]. SOFC is the one that attracts a lot of attention from researchers due to their advantages with high durability, low cost, great efficiency and being environmentally friendly [1,3,4,5]. The combined cycle power plant, the cogeneration of electricity, and residential application are the three primary uses for SOFC. However, due to their high temperature at which it operates, SOFC is not suited for use in portable applications or transportation. In contrast, researchers are currently looking at ways to lower the temperature at which SOFC operates in order to make the technology viable for use in the portable applications such as vehicle, trucks and other support machine [6]. The technology of SOFC also can be applied in military, navy, domestic use and industries. This is because SOFC can be used in our fleet vehicles include cars, trucks, buses, boats and variation other specialized vehicles such as lift trucks and ground support equipment. The main component in SOFC that can affect the cell performance is the electrolyte [2,7]. Solid electrolyte of ceria based has been known as a potential candidate for SOFC due to its excellent electrical properties with high ionic conductivity. However, in order to enhance the SOFC performance co-doping ceria based may further increase the conductivity of solid electrolyte for SOFC as reported in previous studies [7,8]. Iron oxide (Fe_2O_3) is the transition metal that is suggested as a good dopant for enhancing the ionic conductivity as well as to serves as a sintering aid for CeO_2 based electrolytes. This dual purpose feature of Fe_2O_3 makes it a very practical candidate [9]. Moreover, it has lower cost compared to common rare earth dopant. It is has been reported that Fe based material can be used as electrode for SOFC. Therefore, by using Fe as dopant in electrolyte, it might increase the compatibility of the Fe based electrode with Fe doped electrolyte due to adequate valence stability of the Fe-O bond for outstanding redox activity [10]. In addition, it is function as an impurity degreaser at grain boundaries. Besides, the oxidation state of Fe^{3+} can enhance the vacancies of oxygen and ionic conductivity [11]. In order to improve the densification of SOFC electrolyte, transition metal has been proven as a good sintering promoter [12]. In this study, Fe_2O_3 doped $\text{Ce}_{0.8}\text{Sm}_{0.2}\text{O}_{1.9}$ was synthesized. The correlation between structural and electrical properties on those doping was investigated.

MATERIALS AND METHODS

Different ratios of high purity of cerium oxide, CeO_2 (99.9% purity, Acros Organics), samarium oxide, Sm_2O_3 (99.95% purity, Sigma Aldrich) and iron oxide, Fe_2O_3 (96% purity, Sigma Aldrich) were used as a raw materials. The solid solution of $\text{Ce}_{0.8}\text{Sm}_{0.2}\text{O}_{1.9}$, $\text{Ce}_{0.8}\text{Sm}_{0.1}\text{Fe}_{0.1}\text{O}_{1.9}$ and $\text{Ce}_{0.7}\text{Sm}_{0.2}\text{Fe}_{0.1}\text{O}_{1.85}$ are abbreviated as C8S2, C8-S1F1 and C7-S2F1, respectively, were synthesized by conventional solid state reaction method. Those raw materials were weighed according to stoichiometric ratio and mixed homogeneously for 1 h with addition of ethanol by using agate mortar. The

homogenous dried powder was pressed into pellet shape under pressure 3000 psi by using a manual hand press. The green pellet was sintered at 1400 °C, 1450 °C, 1480 °C and 1500 °C for 5 h.

Archimedes' method was used to determine the mass density of the sintered pellet. The sintered pellet was ground into powder for X-ray diffraction (XRD) measurement. The scanning range was between 20° and 90° with Cu K α radiation. XRD analysis was done for phase confirmation as well as evaluation of lattice parameter, unit cell volume and crystallite size. Impedance spectroscopy recorded the ionic conductivity of the sintered pellet. To provide an excellent conductivity measurement, silver paste was coated on both sides of the pellet and heated at 700 °C for 1 h. The measurement was conducted at a temperature range between 300 °C and 800 °C with the increment of 100 °C in the range frequency between 0.1 Hz and 1 MHz [13]. Diameter and thickness of the sample was measured before and after the sample underwent the sintering process to calculate the volume shrinkage.

RESULTS AND DISCUSSION

Phase confirmation and crystal structure analysis

XRD patterns of C8S2 sample sintered at 1400 °C, 1450 °C, 1480 °C and 1500 °C for 5 h are shown in Figure 1. For the sample that was sintered at 1400 °C, the XRD pattern showed mixed phase of CeO $_2$ and Sm $_2$ O $_3$ where peaks due to Sm $_2$ O $_3$ was identified at 32.8°, 47.2° and 55.9°. Meanwhile single phase with fluorite structure and agreed well with reference PDF card 01-075-0157 was obtained for samples that were sintered at 1450 °C, 1480 °C and 1500 °C. C8S2 sample sintered at 1400 °C did not achieve the required sintering temperature because the optimum sintering temperature for C8S2 is between 1450 °C and 1600 °C [4].

Figure 2 shows the XRD patterns for C8-S1F1 sample sintered at 1450 °C, 1480 °C and 1500 °C for 5 h. Sample sintered at 1450 °C has a mixed phase, while single phase was obtained in the sample sintered at 1480 °C and 1500 °C. A single phase was obtained at 1500 °C, but the C8-S1F1 sample start to melt at this temperature. In this case, the optimum sintering temperature for C8-S1F1 sample was 1480 °C.

Figure 3 illustrates the XRD patterns that were obtained by all of the samples that were sintered at 1480 °C. The samples C8S2 and C8-S1F1 were found to be in a single phase however, a secondary phase of Fe $_2$ O $_3$ was discovered in the C7-S2F1 sample. It is reported that, secondary phase might interfere the electrochemical reaction taking place between electrode and electrolyte, which reduces the cell performance [14]. Therefore, 1480 °C was not a suitable sintering temperature for the C7-S2F1 sample to attain the single phase. So, this sample requires a different sintering profile.

Crystal data for all samples is shown in Table 1. As seen in the table, similar lattice parameters and volume were obtained when the sample was co-doping with Sm $_2$ O $_3$ and Fe $_2$ O $_3$. Lattice parameter that was obtained from the other reported research was 0.5414 nm which is slightly similar to the lattice parameter that has been obtained in this study [15]. Even though, Fe $^{3+}$ has smaller radius (0.078 nm) compared to Ce $^{4+}$ which is (0.097 nm) and substitution of Fe $^{3+}$ to Ce $^{4+}$ can lead to the variation in lattice parameters [4,13]. However, crystallite size was increased with Fe $_2$ O $_3$ as secondary dopant.

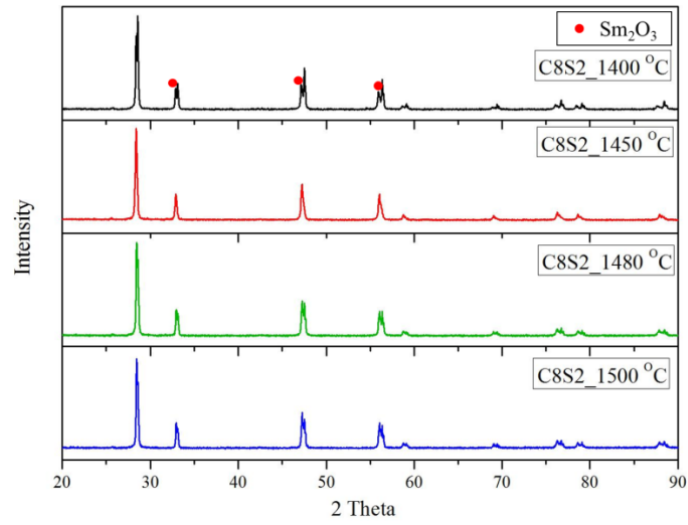


Figure 1. XRD patterns of C8S2 at different sintering temperatures

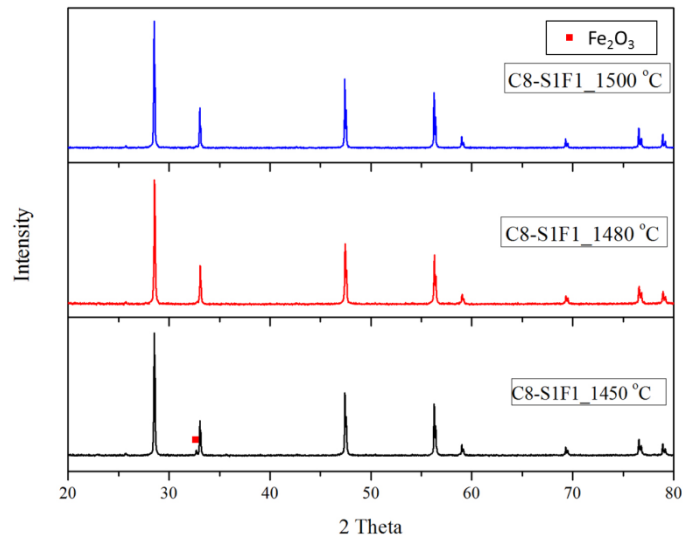


Figure 2. XRD patterns for C8-S1F1 at different sintering temperatures

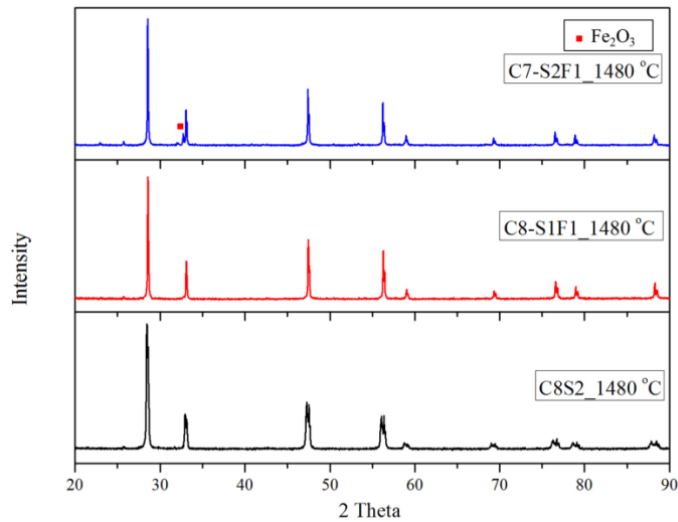


Figure 3. XRD patterns for all samples at optimum sintering temperature

Table 1. Crystal data for all samples

Sample	Lattice parameter, a (nm)	Unit Cell Volume, V (nm ³)	Average Crystallite size, D (nm)	Phase
C8-S2	0.5444	0.1697	52.092	Single
C8-S1F1	0.5422	0.1594	75.233	Single
C7-S2F1	0.5425	0.1597	83.322	Mixed

Electrical Conductivity

Arrhenius plot in Figure 4 shows the total conductivity for the three samples at temperature range between 300 °C and 800 °C. The total conductivity, σ of the sample at different temperature can be obtained by using the equation:

$$\sigma = \frac{L}{SR}, \quad (1)$$

where, L and S represent the sample thickness and area of the sample surface, respectively. R represents resistance.

As can be seen in Figure 4, at lower temperature regions, between 300 °C and 500 °C, the conductivity of the three samples are significantly different, C7-S2F1 possesses the highest value, followed by C8S2, then C8-S1F1. For example at 300 °C, C7-S2F1, C8S2 and C8-S1F1 have conductivity values of 0.0130 $\Omega^{-1}\text{m}^{-1}$, 0.0015 $\Omega^{-1}\text{m}^{-1}$ and 0.00005 $\Omega^{-1}\text{m}^{-1}$, respectively. This result shows that the composition of the sample and the site where Fe dopant occupied remarkably affects the conductivity as reported by Yasin Polat who studied the electrolyte material contain CeO₂, Sm₂O₃ and Bi₂O₃. In that report, the conductivity of the based material depended on the concentration of CeO₂ as doping materials [16].

It has been reported in other ceramic materials with high resistance and low electrical conductivity material affirm with low doping concentration of Fe [17]. Jihai Cheng has stated that conductivity of Sm doped CeO₂ with additional Fe dopant increases when Fe content maximum reaches 10 mol% and further addition decreases the conductivity [9]. In the present study, we reported Fe content at 10 mol %.

Meanwhile, at higher temperature region, above 600 °C, it is found that, the difference of the conductivity values between these three samples become smaller. For instance, this can be clearly observed for the conductivity values at 800 °C, samples seem to be overlapped. Nevertheless, the trend is similar to the lower temperature region where C7-S2F1 shows the highest value, followed by C8S2, then C8-S1F1. From these results, it can be said that Sm and Fe dopant effect on the conductivity of the parent material CeO₂ is profound in the mechanism of ion-vacancy dissociation which occurs at lower temperature, compared to mechanism of ion migration that takes place at higher temperature regions. However, according to Yifeng Zheng, C8S2 with 0.15 mol % of Fe₂O₃ will not improve the C8S2 due to the second phase of Fe₂O₃. Thus, this study on C8-S1F1 did not improved the conductivity of C8S2 even though 0.1 mol % of Fe₂O₃ was added due to the formation of second-phase Fe₂O₃ diminishes the electrochemical property [4].

The Arrhenius equation used to calculate the conductivity data is shown in equation (2):

$$\sigma = \frac{A}{T} \exp\left(-\frac{Ea}{kT}\right). \quad (2)$$

In this equation, E_a is the activation energy for ionic migration, k represents the Boltzmann's constant, T is for absolute temperature and A denotes the pre-exponential factor, which is a constant at a certain temperature range [18]. The activation energy for each sample is shown in Table 2 which is determined from the gradient of the Arrhenius plot. R^2 value represents how good the data were fitted in the gradient line for determination of activation energy, E_a . In this study, all samples achieved R^2 value above 0.975. Jason Fernando states a good R^2 value is above 0.9 [19]. The C8S2 sample has a similar value compared to the previous study with a difference of 0.064 eV. In a previous study, the minimum activation energy required for Sm doped CeO₂ sample was about 0.892 eV [20]. In this study, C7-S2F1 required the lowest activation energy compared to C8S2 and C8-S1F1. Here, the small total activation energy will provide higher conductivity value, which is proven by the conductivity value.

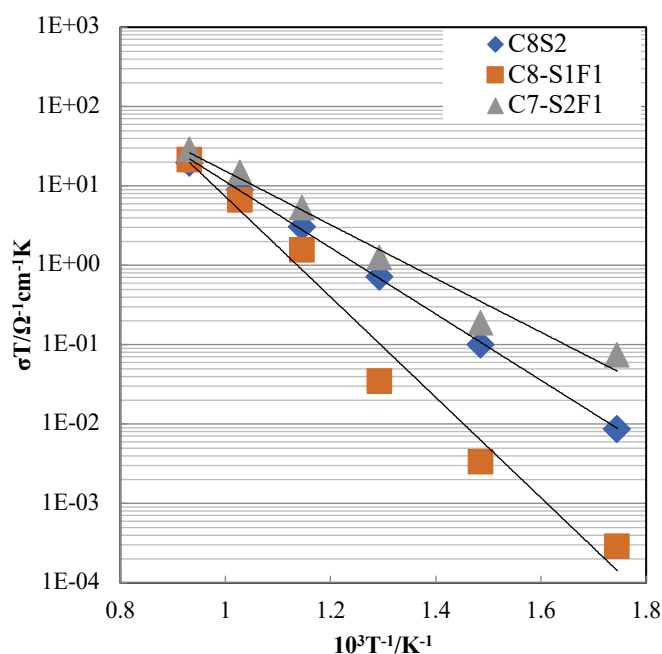


Figure 4. Arrhenius plot of different samples at optimum sintering temperature

Table 2. Total activation energy and value conductivity of different samples

Sample	Total Activation Energy, E_a (eV)	Value of conductivity at 600 °C, σ ($\Omega^{-1}\text{m}^{-1}$)	R^2 Value
C8-S2	0.828	0.350	0.9993
C8-S1F1	1.255	0.180	0.9756
C7-S2F1	0.671	0.613	0.9754

Physical properties

Based on the data obtained from Table 3, the average relative density and volume shrinkage behaviour has been affected by double doping with Sm_2O_3 and Fe_2O_3 . In this study, relative density of the single phase sample and Fe co-doping sample increased about 2.18%. In a previous report, samples with high density generally obtained high ionic conductivity [21]. The samples doped with Fe showed increments in the relative density because this dopant strongly promoted the densification rate of the C8S2 and the viscous flow sintering occurred in the sample [4]. However, the density for Fe co-doping with mixed phase was not yet identified. The difference in volume shrinkage is up 16% and the average volume shrinkage increases by doping with Fe. This is because the small amount of Fe added in the composition increases the effect of the shrinkage [4].

Table 3. Average relative density and volume shrinkage

Sample	Average relative Density (%)	Average Volume shrinkage (%)
C8-S2	97.38	29.99
C8-S1F1	99.40	38.98
C7-S2F1	nil*	46.13

CONCLUSIONS

Fe_2O_3 and Sm_2O_3 co-doped CeO_2 samples were investigated in terms of their crystal structure and ionic conductivity. C8S2 and C8-S1F1 showed optimum sintering temperature at 1480 °C while C7-S2F1 sample required a different sintering profile because a mixed phase was identified at this temperature. The densification of C8S2 can be improved by Fe doping, and the volume shrinkage increases whenever the relative density increases. The conductivity of C8S2 was improved by doping with 10 mol% of Fe_2O_3 with composition of $\text{Ce}_{0.7}\text{Sm}_{0.2}\text{Fe}_{0.1}\text{O}_{1.85}$ (C7-S2F1). C7-S2F1 has conductivity of $0.613 \Omega^{-1}\text{m}^{-1}$ at 600 °C, indicates an improvement approximately 1.8 times compared to sample without Fe doping. The activation energy of C7-S2F1 was 0.671 eV which is the lowest value among synthesized samples. In addition, all synthesized samples in this study show comparable value of density, lattice parameter and unit cell volume. From all the finding, Sm and Fe co-doped CeO_2 can be a promising candidate as electrolyte for SOFC. However, further research need to be performed.

ACKNOWLEDGMENTS

The author would like to acknowledge the support from the Fundamental Research Grant Scheme (FRGS) under a grant number of FRGS/1/2020/STG05/UNIMAP/02/4 from the ministry of Higher Education (MoHE) Malaysia.

REFERENCES

- [1] Nandini Jaiswal, Khagesh Tanwar, Rathod Suman (2019). A brief on ceria based solid electrolytes for solid oxide fuel cells, *Journal of Alloys and Compounds* **781**, 984.
- [2] S. Mekhilef, R. Saidur, A. Safari (2011). Comparative study of different fuel cell technologies, *Renewable and Sustainable Energy Reviews* **16**(1), 981.
- [3] Mandeep Singh, Dario Zappa, Elisabetta Comini (2021). Solid oxide fuel cell: Decade of progress, future perspectives and challenges, *International Journal of Hydrogen Energy* **46**(54), 27643.
- [4] Yifeng Zheng, Ming Zhou, Lin Ge (2011). Effect of Fe₂O₃ on Sm-doped ceria system solid electrolyte for IT-SOFCs, *Journal of Alloys and Compounds* **509**(2), 546.
- [5] Salmie Suhana Che Abdullah, Siti Sarah Ismail (2019). Influence of NiO to SDC ratio on the properties of Ni-SDC cermet prepared via reduction process, *IOP Conf. Ser.: Mater. Sci. Eng.* **701**, 102028.
- [6] Arnab Choudhury, H. Chandra, A. Arora (2013). Application of solid oxide fuel cell technology for power generation, *Renewable and Sustainable Energy Reviews* **20**, 430.
- [7] M.J. Pawar, S.S. Chaure, S.B. Deshmukh (2010). Effect of Co co-doping on the densification and electrical conductivity of Ce_{0.9}Sm_{0.1}O_{2-δ} solid electrolyte, *J. Ceram. Sci. Tech.* **01**(01), 27.
- [8] Yasin Polat, Mehmet An, Yilmaz Dagdemir (2017). Phase stability, thermal, electrical and structural properties of (Bi₂O₃)_{1-x-y}(Sm₂O₃)_x(CeO₂)_y electrolytes for solid oxide fuel cells, *Phase Transitions* **90**(4), 387.
- [9] Jihai Cheng, Changan Tian, Jie Yang (2019). Effects of Fe₂O₃ addition on the electrical properties of SDC solid electrolyte ceramics, *Journal of Materials Science* **30**, 16613.
- [10] Chengsheng Ni, Jun Zhou, Ziye Zhang (2021). Iron-based electrode materials for solid oxide fuel cells and electrolyser, *Energy & Environmental Science* **14**, 6287.
- [11] D.L. Maricle, T.E. Swarr, S. Karavolis (1992). Enhanced ceria-a low-temperature SOFC electrolyte, *Solid State Ionics* **52**, 173.
- [12] B. Johar, N.A. Zaili (2016). Fe doped 8YSZ at different compositions for solid electrolyte in solid oxide fuel cells, *MATEC Web of Conferences* **78**, 01102.
- [13] Guixiang Hua, Xifeng Ding, Wenliang Zhu, Jianfei Li (2015). Enhanced ionic conductivity of Sm_{0.2}Ce_{0.8}O_{2-δ} electrolyte for solid oxide fuels cells through doping transition metals, *Journal of Master Science: Materials in Electronics* **26**, 3664.
- [14] X. Sun, S. Deng, Y. Xia, B. Li, Y. Tian, J. Chen (2022). Effect of TiO₂ as an additive on the sintering performance of Sm-doped CeO₂ based electrolyte for solid oxide fuel cells, *Front. Chem* **10**, 1034993.
- [15] Hikmet Okkay, Mahmut Bayramoglu (2013). Ce_{0.8}Sm_{0.2}O_{1.9} synthesis for solid oxide fuel cell electrolyte by ultrasound assisted co-precipitation method, *Ultrasonic Sonochemistry* **20**(3), 978.
- [16] Alena Borisovna Kharissova, Moises Hinojosa Rivera, Oxana V. Kharissova (2018). Synthesis and characterization of CeO₂ doped with Sm₂O₃ and Eu₂O₃ for the use in SOFCs, MRS Advance, *Materials Research Society* **3**, 1855.

- [17] Arvind Kumar, Vijayeta Pal, S.K. Mishra (2016). Effect of Fe doping on structural and impedance properties of PZTFN ceramics, *AIP Conf. Proc.* **1728**, 020594.
- [18] Yifeng Zheng, Haitao Gu, Han Chen (2009). Effect of Sm and Mg co-doping on the properties of ceria-based electrolyte materials for IT-SOFCs, *Materials Research Bulletin* **44**(4), 775.
- [19] Jason Fernando (2021). R-Squared Formula, regression and interpretations, Investopedia. <https://www.investopedia.com/terms/r/r-squared.asp>
- [20] Yen Pei Fu, Shaw Bing Wen, Chi Hua Lu (2008). Preparation and characterization of samarium-doped ceria electrolyte materials for solid oxide fuel cells, *Journal of American Ceramics Society* **91**(1), 127.
- [21] Yin Shilong, Li Mengnan, Zeng Yanwei (2014). Study of $\text{Sm}_{0.2}\text{Ce}_{0.8}\text{O}_{1.9}$ (SDC) electrolyte prepared by a simple modified solid-state method, *Journal of Rare Earth* **32**(8), 767.